J.Natn.Sci.Foundation Sri Lanka 2020 48 (3): 305 - 313
DOI: http://dx.doi.org/10.4038/jnsfsr.v48i3.9026

RESEARCH ARTICLE

Effect of precipitate size distribution on hardness of aluminium 6063 alloy

LWUR Dilrukshi* and GIP De Silva
Department of Materials Science and Engineering, Faculty of Engineering, University of Moratuwa, Moratuwa.

Submitted: 11 October 2019; Revised: 31 March 2020; Accepted: 29 May 2020

Abstract: In this study, the effects of precipitate size and size distribution on the hardness of Al 6063 alloy were examined. Al 6063 samples were subjected to a solution treatment at 530 °C for 4 hours and quenched in water followed by storing in freezer (-18 °C) to prevent natural ageing. Ageing treatment was done at 190 °C for 135, 180, 225, 270 and 315 minutes. Precipitates distributed in the matrix were identified as Fe-Si-rich and Fe-Si-Mg-rich precipitates by performing Scanning Electron Microscope/Energy Dispersive Spectroscopy (SEM/EDS) analysis. Number of precipitates, average size and the area covered by precipitates were calculated by Image J software based on the precipitates observed in SEM images. For all heating profiles, precipitate size was less than 3.2 µm. Maximum hardness of 143.90 HV was achieved for 270-minutes ageing time. A significant decrease in hardness was evident when the particles were coarsening above 1.5 µm, possibly due to overageing for ageing time beyond 270 min.

Keywords: Age hardening, Al 6063 alloy, hardness, precipitate size distribution.

INTRODUCTION

Aluminium (Al) is the most abundant metal on the Earth crust containing 8 % of the weight of the Earth's solid surface. Aluminium 6063 alloy consists of Mg (0.45–0.90 wt %) and Si (0.2–0.6 wt %) as its major alloy elements (Couper *et al*., 2010). It is extensively used for structural applications such as partitioning, windows, door frames, ladders and bars of varying cross-sections. In addition, it has been identified as a marine grade alloy because of its excellent corrosion resistance in marine environments. The high strength-to-weight ratio has made it very attractive to aviation and automobile industries as well. Its corrosion resistance, high strength and excellent extrudability make it an excellent structural material.

Al 6063 alloy has been subjected to a precipitation hardening treatment to improve its hardness and strength up to a required level that is dependent on the components to be produced (Cavazos & Colãs, 2003). Thus, wide-ranging knowledge regarding evolution of microstructure during precipitation hardening and their effect on mechanical properties are critically focused in previous research (Cavazos & Colãs, 2003; Nandy *et al*., 2015). Current research on precipitation hardening of Al 6063 alloy have studied the effect of chemical composition and heat treatment profile either individually or in combination to gain the required level of strength and hardness. Yildirim & Özyürek (2013) found the effect of magnesium content on the strength and hardness of Al 6063 alloy.

The quench sensitivity of aluminium alloys has been studied by Cavazos & Colãs (2003). The study concluded that final hardness was sensitive only for cooling rate lower than 10 ^{0}C/s after solution treatment due to incipient precipitation. Li *et al*. (2013) repeated the same experiments using a salt bath instead of water as the quenching medium and found that the critical temperature range of 410–300 ^{0}C is more susceptible for incipient precipitation. This is an important result for the

* Corresponding author (dilrukshiur80@gmail.com; https://orcid.org/0000-0003-2531-9483)

This article is published under the Creative Commons CC-BY-ND License (http://creativecommons.org/licenses/by-nd/4.0/). This license permits use, distribution and reproduction, commercial and non-commercial, provided that the original work is properly cited and is not changed in anyway.

aluminium extrusion industry as cooling rate needs to be controlled specially within the above temperature range.

Siddiqui *et al*. (2000) studied the ranges of age hardening process parameters and their combinations to obtain the different sets of tensile strength, yield strength and hardness. The best combination in terms of applications - tensile strength (150 MPa), yield strength (140 MPa) and hardness (68 RB), was obtained at 175 ^{O}C for 8–10 hour ageing time.

Precipitates/particles strengthen the alloy by acting as obstacles to dislocation motion by 'cutting through (shearing)' and 'bowing and bypassing' mechanisms (Kulkarni *et al*., 2004).

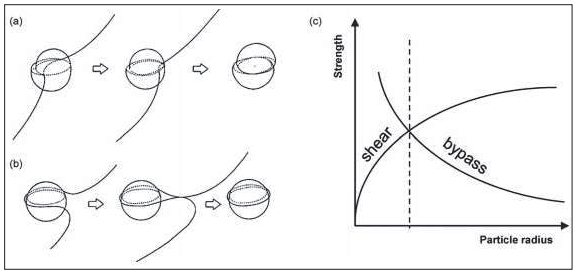

Figure 1: Schematic illustration of (a) cutting through and (b) bowing and bypassing; (c) relationship between strength vs precipitate radius (Sjölander & Seifeddine, 2010)

There is an elastic stress existing in the matrix around the precipitate due to difference lattice parameter relative to the matrix area, especially at the early stage of precipitation where particles are smaller and less hard. Under this condition, metal hardening would predominantly occur by cutting through mechanism. In addition, coherency and modulus hardening and, chemical and ordering strengthening contribute to the hardening of metal matrix (Guo & Sha,2005). For a longer ageing time, inter-particle space is increased in resulting coarsening of precipitates; this condition leads to the bowing and bypass mechanism.

According to previous research (Jacobs, 1999; Kulkarni *et al*., 2004) cutting through mechanism significantly affect increasing the hardness relative to the bowing and bypassing. However, bowing and bypassing associated with coarser particles make the structure more brittle while reducing the hardness and strength. This phenomenon is schematically illustrated in Figure 1.

The degree of strengthening is determined by the particle size, size distribution as well as inter-particle spacing. In this work, all types of precipitates distributed in the matrix (solid solution) are considered as the second phase and that is denoted as β. Research (Gao *et al*., 2009; Lillywhite *et al*., 2012; Asensio-Lozano *et al*., 2014) has shown that cutting through mechanism becomes predominant with higher percentage of particles in the size range of R_1 (0.00–0.2 μm) and bowing and bypassing mechanism becomes predominant within the particle size range of R_2 (0.2–1.5 μm). Further, they have shown that both mechanisms could be activated within the range of R_2 (0.2–1.5 μm).

Research has been carried out regarding dislocation interaction with precipitate obstacles in age hardened Al alloys through computational simulations. For a given ageing temperature, increasing the average radius of precipitates while maintaining constant volume fraction would initially increase the strength to maximum followed by a diminishing in strength (over-ageing) (Mohles *et al*., 1999). This type of system follows the Ostwald Ripening behaviour. The larger particles (energetically favoured) were grown further by dissolving small particles while minimizing the total area covered by precipitates. In 1958, Lifshitz and Slyozov derived a mathematical model for such a system to evaluate the distribution of the particle radii, presently known as LWS theory.

Mechanical properties after application of ageing treatment depend on the size and size distribution of the precipitates being formed, which depends on processed time and temperature (Cavazos & Colãs, 2003). This work is focused on studying the variation of hardness of Al 6063 alloy with the precipitate size distribution in different size ranges, under the increase of ageing time.

METHODOLOGY

Original Al 6063 alloy samples homogenised at 570 ^{o}C for 2.5 h were obtained from a local Al products manufacturing company. Chemical analysis was performed by spark emission spectrometer to assure the chemical composition and results are shown in Table 1.

Table 1: Chemical analysis of Al 6063 alloy

Element	Si	Mg	Fe	Cu	Mn	Other Minor Elements	Al
Wt. %	0.42	0.47	0.53	0.01	0.02	0.25	98.3

Samples having the size of 20 mm × 20 mm × 10 mm were used for the heat treatment process. The samples were subjected to a solution treatment for 4 h at 530 ^{0}C in a programmable muffle furnace, followed by quenching in water. The quenched samples were immediately transferred to freezer (-18 ^{0}C) to avoid natural ageing at room temperature (Siddiqui *et al*., 2000). Ageing was done at 190 ^{0}C for 135,180, 225, 270 and 315 min in the same furnace. Two samples were heat treated for each ageing time mentioned above. Vickers hardness was performed as per ASTM E92 (5 kgf, loading speed 70 µm/s, time 15s) and hardness values were calculated by taking the average of five readings for each ageing time.

Specimens having the dimensions of 10 mm × 10 mm × 10 mm were made by using ISOMET Low Speed Saw (oil cutting) and those were cleaned with ethanol (10 min) using ultrasonic cleaner. These specimens were used for the SEM/EDS analysis to ensure the particle types in terms of chemical composition. Observations were performed under BSD mode with current-100 µA, EHT-20 KV and ×5000 magnifications. Images were captured using four specimens belonging to each ageing time and 10 different areas were randomly selected from each specimen to provide a sufficient graphical characterisation for precipitates distribution. These image sets were analysed using Image J software to calculate the number of precipitates, average size and area covered by precipitates. Percentage of precipitates belonging to different size ranges - R_1 (0.0–0.2 µm), R_2 (0.2–1.5 µm) and R_3 (> 1.5 µm) were calculated using curve fitting method.

RESULTS AND DISCUSSION

Application of heat treatments

Al 6063 alloy samples subjected to solution treatment as shown in Figure 2 were age hardened at 190 ^{0}C for 135, 180, 225, 270 and 315 min (t_x) to study the variation of precipitate size and size distribution and its effect on hardness. Parameters of the heating cycle were decided based on the pseudo-binary phase diagram of Al 6063 alloy in Figure 3 (Asensio-Lozano *et al*., 2014).

Microstructure examination and identification of precipitate types

Heat treated specimens of five different heating profiles were then transferred to microstructure examination. SEM images captured from specimens showed that particles with various sizes were distributed in the matrix (α phase) as shown in Figure 4.

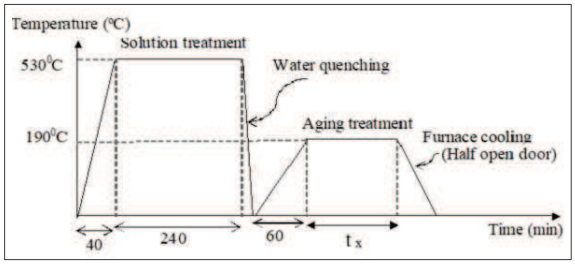

Figure 2: Heat treatment cycle applied to Al 6063 alloy samples

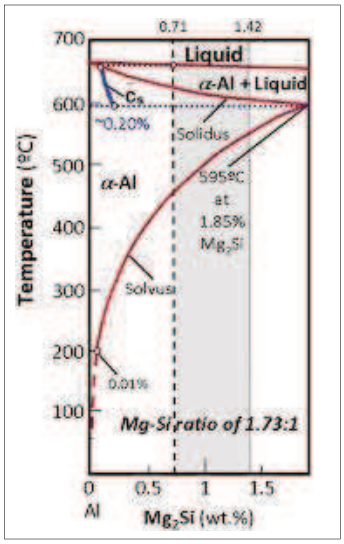

Figure 3: Pseudo-binary phase diagram for Al 6063 alloy

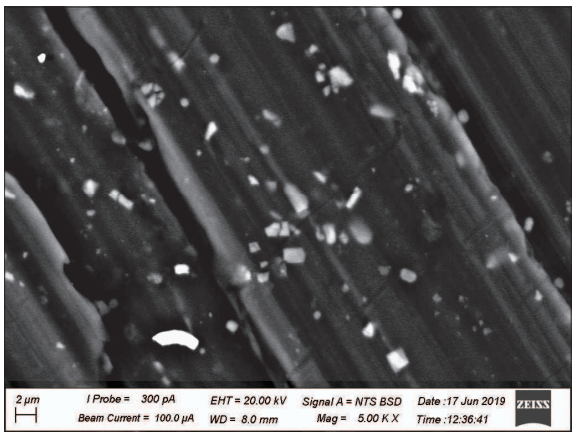

Figure 4: Al 6063 alloy solution treated at 530 ^{0}C for 4 hours, quenched in water and aged at 190 ^{0}C for 180 minutes

In this work, identification of the precipitate/particle types were carried out irrespective of ageing time periods. Ten SEM images were selected from each specimen set related to different ageing times for SEM/EDS analysis of precipitates to ensure their chemical composition in terms of Mg/Al, Si/Al and Fe/Al weight ratios. Element weight ratio relative to the Al content is calculated inside and outside the particles (background/matrix). Two types of precipitates were identified as Si-Fe rich and Mg-Si-Fe-rich precipitates based on the above-mentioned analysis. The method of SEM/EDS analysis of these two precipitate types are explained as follows.

As per Table 2, it is obvious that Si/Al and Fe/Al element weight ratios are significantly higher inside the precipitates relative to the background. Therefore, it could be concluded that those are Si-Fe rich precipitates. Likewise, based on the results shown in Table 3, those precipitates could be identified as Mg-Si-Fe-rich precipitates.

Table 2: Element weight ratios based on EDS results of Figure 5

Element weight ratio (element/Al) ×100%	Inside particle (5a)	Inside matrix (5b)
Mg/Al	2.2	2.1
Si/Al	4.2	0.5
Fe/Al	11.5	0.0
Al content	84.8	97.5

Table 3: Element weight ratios based on EDS results of Figure 6

Element weight ratio (element/Al) ×100%	Inside particle (6a)	Inside matrix (6b)
Mg/Al	2.1	0.6
Si/Al	6.0	1.1
Fe/Al	26.1	1.3
Al content	74.5	97.5

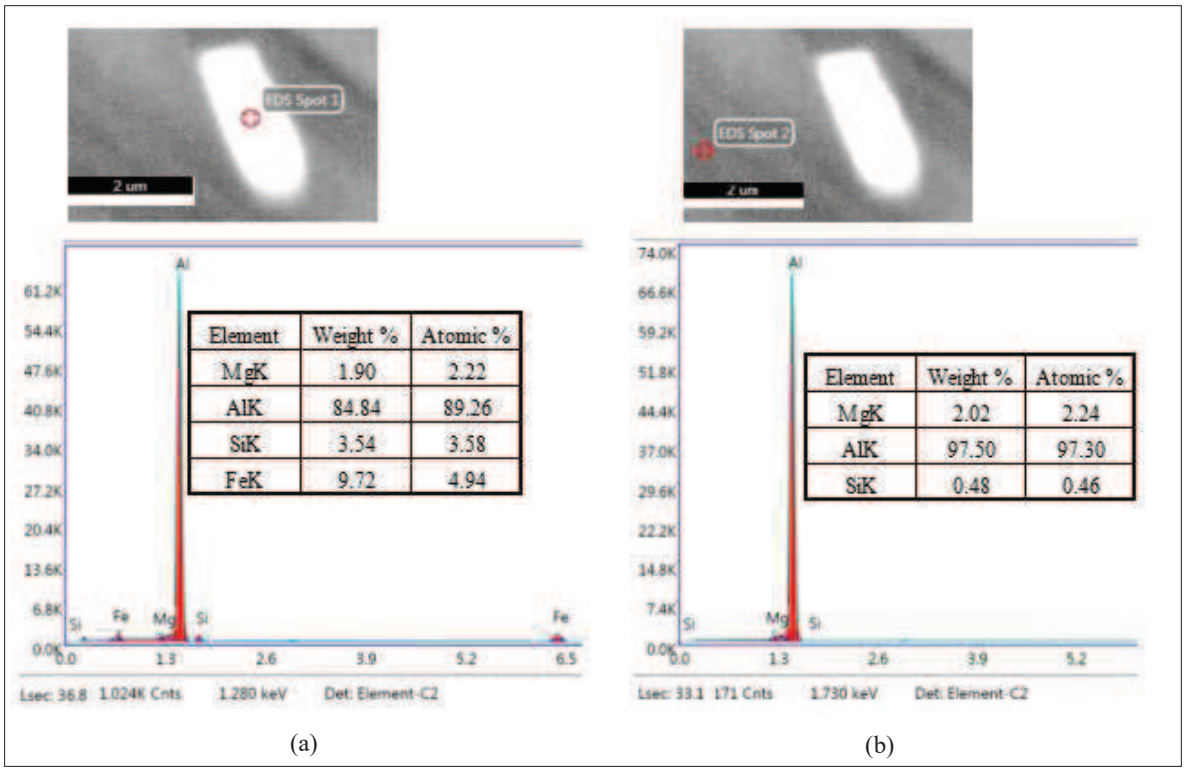

Figure 5: SEM/EDS results of (a) inside and (b) outside of the precipitate formed under ageing at 190 ^{0}C for 135 minutes

These types of second phase particles in age hardened Al 6063 alloy had been identified by previous researchers. Precipitates such as β-Al_5FeSi,Al_{15}(Mn,Fe)3Si and π-$Al_8Mg3FeSi_6$ were identified by Kliauga *et al*. (2008) as precipitate colonies and they further revealed some Fe-rich precipitates. Both Si-rich and Fe-rich precipitates were investigated by Ma *et al*. (2008). Moreover, they have studied the influence of precipitate types on mechanical properties of Al 6063 alloy.

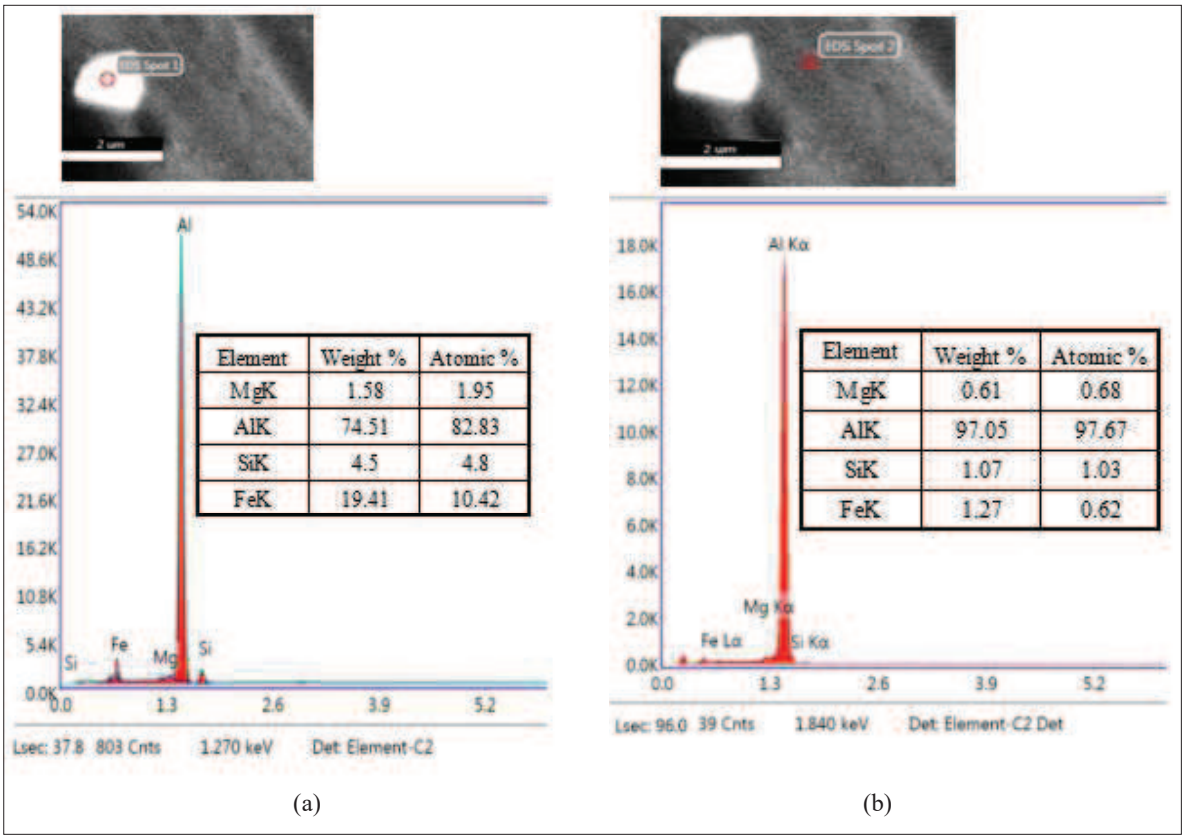

Figure 6: SEM/EDS results of (a) inside and (b) outside of the precipitate formed under ageing at 190 ^{0}C for 315 minutes

Analysis of precipitate size and their distribution

SEM images comprising distributed particles were analysed using Image J (Image Processing and Analysis in Java) software.

Each image was scaled and duplicated to relevant specific areas (50 µm × 30 µm), and thresholded (Figure 7). All the sets of selected images for each ageing time period were analysed as shown in Figures 7 and 8. Average number of particles, their sizes and percentage of area covered by particles per specific area (50 µm × 30 µm) were calculated for each ageing time period, and the results are summarised in Figure 9.

Effect of precipitate size distribution on hardness

As shown in Figure 9, for the ageing time of 315 min, average size of particles is increased while the average number and percentage of area covered by precipitates are reduced, relative to the variation occurred from 135 to 270 min. This behaviour could have possibly occurred due to the phenomenon of overageing; that is coarsening of precipitates beyond a certain limit, absorbing dissolved

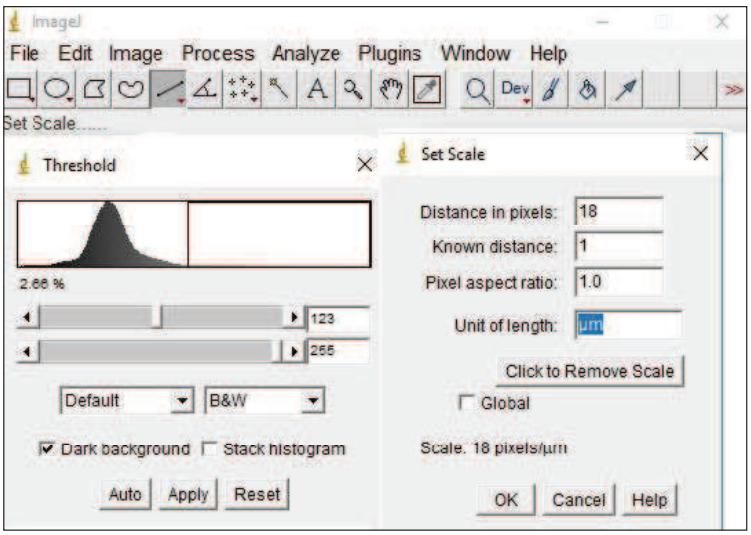

Figure 7: Image J- thresholding and scale functions

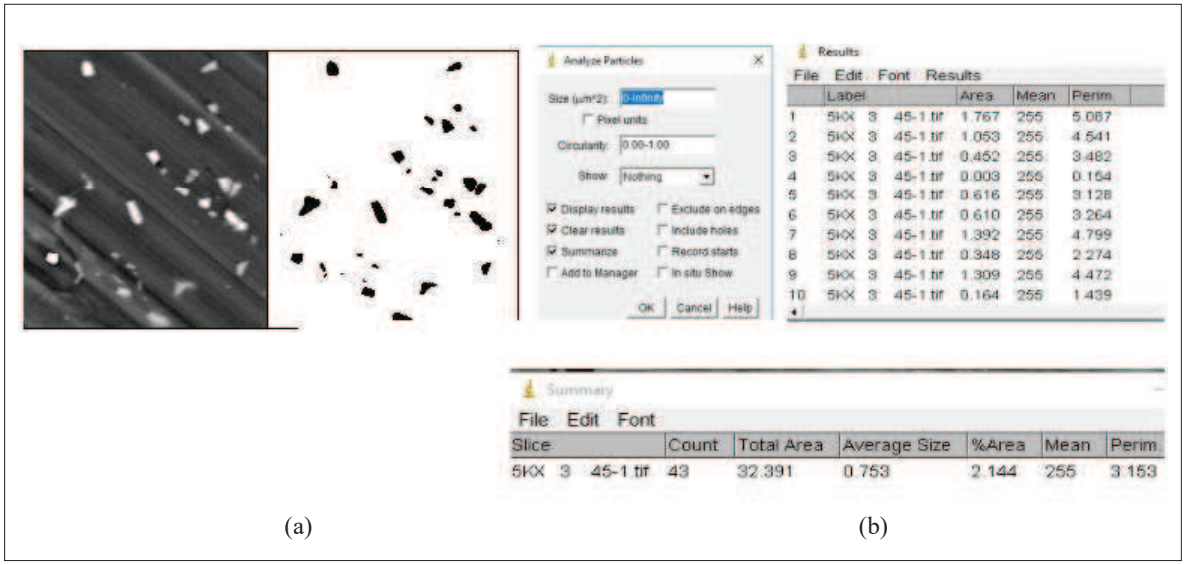

Figure 8: (a) Original and thresholded SEM image of a specimen age hardened for 135 min; (b) data analysis procedure

small meta-stable precipitates. These coarsened particles lead to the development of highly stressed areas in particle-matrix interface, and further this phenomenon leads to the reduction of hardness and strength of the alloy sample. This explanation is justified by the reduction of hardness at 315 min while that is increased from 135 to 270 min (Figure 10).

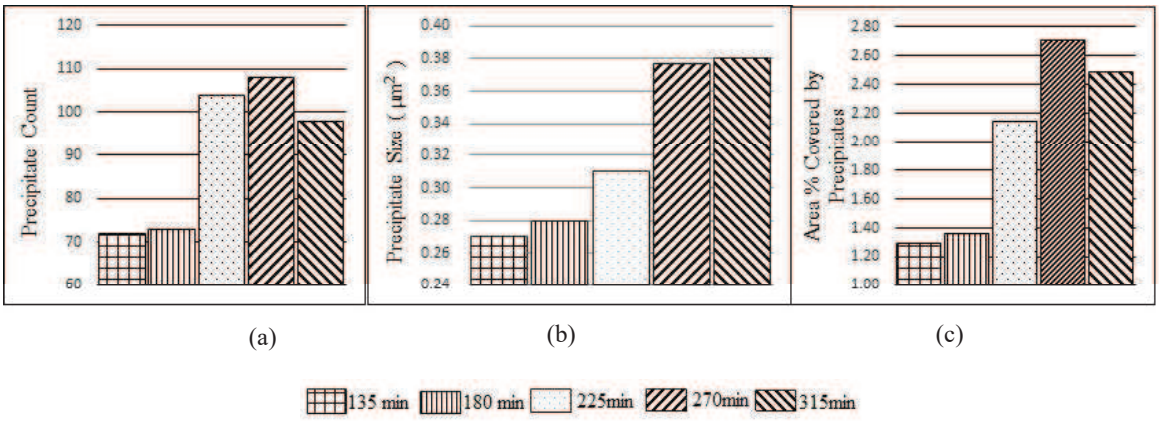

Figure 9: (a) Average number; (b) average size and (c) percentage of area covered by precipitates for specific area (50 μm × 30 μm)

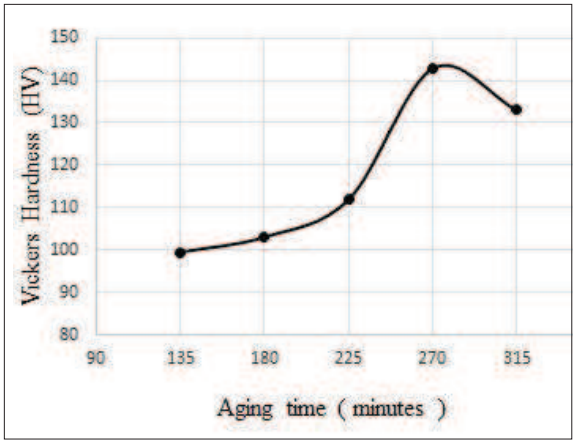

Figure10: Vickers hardness vs. ageing time

Table 4: Vickers hardness of samples aged at different ageing times

Ageing time (minutes)	HV
135	99.4
180	103.0
225	112.9
270	143.9
315	133.0

Table 5: Percentage of particles in different size ranges

Ageing time (minutes)	0.00–0.2 μm R1	0.2–1.5 μm R2	1.5 μm < R3
135	51.0	43.8	5.2
180	56.4	38.6	5.0
225	66.0	29.5	4.5
270	51.5	46.8	1.7
315	50.7	42.7	6.6

The initial increase in hardness occurred due to the hindrance of dislocation by precipitates formed during ageing treatment, especially precipitate size (diameter) up to around 1.5 μm (R_1 + R_2) as explained under the introduction. The percentage of precipitates belonging to each range (R_1, R_2 and R_3) was calculated using a cumulative curve by curve fitting method and the results are summarised in Table 5.

According to the theories and available reports of hardening mechanisms (Jacobs *et al*.,1999; Kulkarni *et al*., 2004), the combination of cutting through, and 'bowing and bypassing' mechanisms play a major role for getting a significant improvement of hardness in Al 6063 within the particle size ranges of R_1 and R_2 (Cavazos & Colãs, 2003; Nandy *et al*., 2015). Concluding all remarks, hardness vs percentage of precipitates belonging to ranges of R_1 and R_2 were plotted as shown in Figure 11.

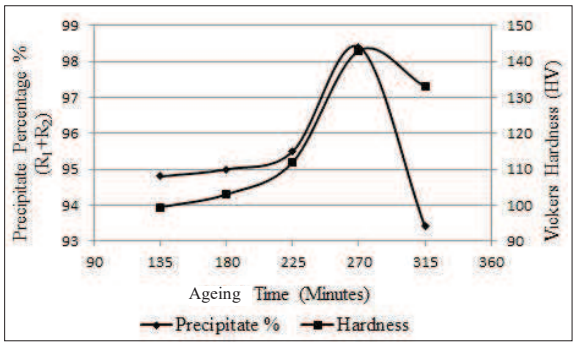

Figure 11: Variation of percentage of precipitates within ($R_1 + R_2$) and hardness with ageing time

As shown in Figure 11, percentage of precipitates within the particle size range of ($R_1 + R_2$) increased up to an ageing time of 270 min and a continuous increase of hardness is obtained accordingly. The highest percentage of precipitates within ($R_1 + R_2$) is 98.3 % and the maximum hardness of 143.9 HV was recorded at an ageing time of 270 min (Figure 11). Moreover, at the ageing time of 315 min, a significant increase of percentage of precipitates above 1.5 µm (R_3), that is 6.6 %, was recorded relative to the ageing time 135 – 270 min (Table 5). Therefore, this reduction of hardness at the ageing time of 315 min could have occurred due to the phenomenon of overageing. The significance of this study is the experimental results shown in Figure 11 clearly explaining the variation of hardness of Al 6063 alloy with the precipitate size distribution in different ranges, under the increase of ageing time.

CONCLUSION

SEM/EDS examination showed that secondary phase precipitates formed at all heating profiles belong to two types of precipitates, as Si-Fe rich and Mg-Si-Fe-rich precipitates.

Percentage of precipitates within the particle size range of 0.0 – 0.2 µm (R_1) and 0.2 – 1.5 µm (R_2) increased up to the ageing time of 270 minutes and the increase of hardness occurred accordingly. The highest percentage of precipitates within ($R_1 + R_2$) is 98.4 % and the maximum hardness of 143.9 HV was recorded at the ageing time of 270 min. Moreover, at this point, percentages of precipitates belong to three different size ranges were 51.5 %, 46.8 % and 1.7 % for 0.0–0.2µm (R_1), 0.2–1.5 µm (R_2) and above1.5 µm (R_3), respectively.

A significant decrease in hardness was evident when the particles are coarsening above 1.5 µm, possibly due to overageing, for the ageing time beyond 270 minutes. At 315 min, percentage of precipitates above 1.5 µm is 6.6 % which is a significant increase relative to the ageing time of 135–270 min.

This study clearly explains the variation of hardness of Al 6063 alloy with precipitate size distribution in different ranges, with the increase of ageing time.

Acknowledgement

The authors thank the academic and non-academic staff of the Department of Materials Science and Engineering, University of Moratuwa and the Senate Research Council (SRC/ST/2018/27) grant of University of Moratuwa for financial assistance. The authors also acknowledge Alumex (Pvt) Ltd. for providing samples and technical assistance.

REFERENCES

Asensio-Lozano J., Suárez-Peña B. & Voort G.F.V. (2014). Effect of processing steps on the mechanical properties and surface appearance of 6063 aluminium extruded products. *Materials* **7**(6): 4224–4242. DOI: https://doi.org/10.3390/ma7064224

Cavazos J.L. & Colás R. (2003). Quench sensitivity of a heat treatable aluminium alloy. *Materials Science and Engineering A* **363**(1–2): 171–178. DOI: https://doi.org/10.1016/S0921-5093(03)00616-6

Couper M.J. (2010). Selecting the optimum Mg and Si content for 6xxx series extrusion alloys. *Proceedings of the 12th International Conference on Aluminium Alloys*, September 5–6, Yokohama, Japan, The Japan Institute of Light Metals, pp. 149–154.

Gao R., Stiller K., Hansen V., Oskarsson A. & Danoix F. (2009). Influence of ageing conditions on the microstructure and tensile strength of aluminium alloy 6063. *Materials Science Forum* **396–**402: 1211–1216. DOI: https://doi.org/10.4028/www.scientific.net/msf.396-402.1211

Guo Z. & Sha W. (2005). Quantification of precipitation hardening and evolution of precipitates. *Materials Transactions* **43**(6): 1273–1282. DOI: https://doi.org/10.2320/matertrans.43.1273

Jacobs M.H. (1999). 1204 Precipitation hardening. *TALAT Lecture*. The University of Birmingham, UK

Kliauga A.M., Vieira E.A. & Ferrante M. (2008). The influence of impurity level and tin addition on the ageing heat treatment of the 356 class alloy. *Materials Science and Engineering A* **480**(1–2): 5–16. DOI: https://doi.org/10.1016/j.msea.2007.07.091

Kulkarni A.J., Krishnamurthy K., Deshmukh S.P. & Mishra

R.S. (2004). Effect of particle size distribution on strength of precipitation-hardened alloys. *Journal of Materials Research* **19**(9): 2765–2773.
DOI: https://doi.org/10.1557/jmr.2004.0364

Li H.Y., Zeng C.T., Han M.S., Liu J.J. & Lu X.C. (2013). Time-temperature-property curves for quench sensitivity of 6063 aluminium alloy. *Transactions of Nonferrous Metals Society of China (English Edition)* **23**(1): 38–45.
DOI: https://doi.org/10.1016/S1003-6326(13)62426-7

Lifshitz I.M. & Slyozov V.V. (1961). The kinetics of precipitation from supersaturated solid solutions. *Journal of Physics of Chemistry of Solids* **19**: 35–50.
DOI: https://doi.org/10.1016/0022-3697(61)90054-3

Lillywhite S.J., Prangnell P.B. & Humphreys F.J. (2012). Interactions between precipitation and recrystallisation in an Al-Mg-Si alloy. *Materials Science and Technology* **16**(10): 1112–1120.
DOI: https://doi.org/10.1179/026708300101507037

Ma Z., Samuel A.M., Samuel F.H., Doty H.W. & Valtierra S. (2008). A study of tensile properties in Al-Si-Cu and Al-Si-Mg alloys: effect of β-iron intermetallics and porosity. *Materials Science and Engineering A* **490**(1–2): 36–51.
DOI: https://doi.org/10.1016/j.msea.2008.01.028

Mohles V., Rönnpagel D. & Nembach E. (1999). Simulation of dislocation glide in precipitation hardened materials. *Computational Materials Science* **16**(1–4): 144–150.
DOI: https://doi.org/10.1016/s0927-0256(99)00056-7

Nandy S., Kumar K. & Das D. (2015). A process model to predict yield strength of AA6063 alloy. *Materials Science and Engineering A* **644**(October 2017): 413–424.
DOI: https://doi.org/10.1016/j.msea.2015.07.070

Siddiqui R.A., Abdullah H.A. & Al-Belushi K.R. (2000). Influence of ageing parameters on the mechanical properties of 6063 aluminium alloy. *Journal of Materials Processing Technology* **102**(1): 234–240.
DOI: https://doi.org/10.1016/S0924-0136(99)00476-8

Sjölander E. & Seifeddine S. (2010). The heat treatment of Al-Si-Cu-Mg casting alloys. *Journal of Materials Processing Technology* **210**(10): 1249–1259.
DOI: https://doi.org/10.1016/j.jmatprotec.2010.03.020

Yıldırım M. & Özyürek D. (2013). The effects of Mg amount on the microstructure and mechanical properties of Al - Si - Mg alloys. *Materials and Design* **51**(2013): 767–774.
DOI: https://doi.org/10.1016/j.matdes.2013.04.089